TRACE ELEMENT AND MICRO-MINERAL COMPOSITION OF SOME SELECTED ANHYDRITE SAMPLES FROM SAINT GHISLAIN DRILL HOLE (HAINAUT, BELGIQUE)

by Ronny VANDELANNOOTE, Luc VAN 'T DACK and

Renaat GIJBELS *

ABSTRACT. - Trace element analysis of selected anhydrite samples from the Saint-Ghislain drill hole (Namur basin, Hainaut, Belgium) revealed them to consist of rather pure $CaSO_4$ with F, Mg, Al, Si, Sr and Ba as main impurities. Detailed electron microprobe analysis showed that in the sample from 2030 m depth, re-mainders of soluble salts (sylvite) were present. This proves that at least locally, evaporites have developed beyond the gypsum and halite precipitation phase. The fact that no massive halite deposits were found so far, supports the hypothesis that the karstic cavities and breccias in the Visean strata may indeed have been formed by the dissolution of the more soluble salts which were originally present in the evaporitic series. The sample from 2352 m depth contains significant amounts of baryte. Its origin is however not clear and different mechanisms can be invoked for explaining its presence. More detailed isotopic and chemical information is needed for this purpose. Such data may possibly also indicate whether there is some similarity with other more massive baryte deposits of the same age (e. g. Fleurus).

RESUME. - L'analyse chimique de traces d'éléments dans plusieurs échantillons anhydritiques du sondage de Saint-Ghislain (Synclinorium de Namur, Hainaut, Belgique) a démontré qu'ils sont constitués d'une phase assez pure, contenant des impuretés minimes comme F, Mg, Al, Si, Sr et Ba. Une analyse plus approfondie par microsonde électronique a mis en évidence la présence de sylvite (échantillon provenant d'une profondeur de 2030 m). Ceci nous fait penser qu'au moins, très localement, des phases évaporitiques se sont développées au delà de la précipitation du gypse et de l'halite. La disposition des dépôts massifs d'halite supposés d'être présents à l'origine dans les formations évaporitiques de Saint-Ghislain, est évoquée pour expliquer la formation des cavités karstiques et des brèches du Viséen. L'échantillon prélevé à 2352 m de profondeur contient des quantités assez importantes de barytine. Son origine n'est pas claire et plusieurs réactions peuvent être mentionnées pour expliquer sa présence. Des analyses isotopique et chimique peuvent fournir plus d'information à ce sujet et peuvent indiquer s'il y a des similitudes avec d'autres dépôts de barytine du même âge (par exemple Fleurus).

INTRODUCTION.

In the Franco-Belgian part of the Hercynian orogeny, Dinantian (Lower Visean) evaporitic series were drilled twice : at Saint-Ghislain, 760 m thick, mainly anhydritic layers were encountered at depths between 1900 and 2740 m (DELMER et al., 1981); at Epinoy (Cambrai, France) these evaporitic series have a thickness of 1000 m (LAUMONDAIS et al., 1984). The anhydrite is the transformation product of primary gypsum, which precipitated by evaporation of waters from marine origin. Many secondary mineralogical transformations and tectonic deformations have been invoked for explaining the different facies encountered nowadays (ROUCHY et al., 1984). The Visean strata also contain important water bearing collapse breccias and karstic cavities. These structures are believed to have been formed partially by the dissolution of more soluble salts (such as halite) which are assumed to have been present in association with anhydrite formation (DELMER et al., 1981). However, none of these salts (halite, sylvite,...) have been positively identified, only some cubic (halite ?) crystals pseudomorphised into calcite or dolomite were detected in Visean breccias. In order to elucidate some of these problems, we applied trace element and detailed micromineralogical analyses to some selected anhydrite samples. Even though only 11 samples have been investigated, this work led to some interesting observations.

EXPERIMENTAL.

Instrumental neutron activation analysis and energy-dispersive X-ray fluorescence analysis were applied to crushed aliquots of samples. The procedures have been described in detail by BLOMMAERT (1983) and by VAN GRIEKEN et al. (1979). In total 11 samples were investigated, their exact location as well as a simplified geological cross section is shown in figure 1 (adapted from ROUCHY et al., 1984). Selected samples were studied in more detail using a JEOL electron microprobe (Superprobe 733), equipped with an X-ray detection system, permitting local chemical analysis of the sample.

RESULTS AND DISCUSSION.

Although the applied multielemental analytical techniques are very sensitive, only a very limited number of impurities could be detected. Table 1 gives the results expressed in μg/g sample. The main impurities are F (probably fluorite), Mg, Al and Si (probably a variety of clay silicates) and Sr and Ba (probably celestite and baryte). For comparison, the analytical data for the thermal water of Saint-Ghislain (for both the aqueous phase and the suspended matter) are also shown in Table 1. These results have been described in detail by BLOMMAERT et al. (1983). It appeared that this thermal water is in thermodynamic equilibrium with minerals such as anhydrite, calcite, fluorite, celestite,

baryte and siderite; most of them were indeed reported to be present in the evaporitic strata (ROUCHY et al., 1984). It is also interesting to note the higher Na/Ca, K/Ca Cl/Ca and HCO_3^-/Ca ratios in the thermal waters as compared to evaporites; the origin of these elements can, however, not unambiguously be stated since water encounters many different environments during its circulation. Note also that the same elements (e.g. F, Al, Sr and Ba) found in the anhydrite are present in the water at rather high concentration. Besides, some chalcophile elements were detected (Fe, Cu, Zn and Sb) which suggests that the water has come in contact with some locally present base metal sulfide mineralizations.

From Table 1, one can see that especially the anhydrite samples from 2030 and 2352 m depth behave anomalously, the former has high concentrations of F, Na, Mg, Al, Si, K and Fe, while the latter has a high Ba content. We decided therefore to investigate both samples in more detail using electron microprobe X-ray analysis.

As could be predicted from the bulk chemical analysis, the sample from 2030 m depth consists mainly of anhydrite with some carbonate phases also being present. Much more interesting is the presence of sylvite micro crystals in this sample. In some cases, these crystals are imbedded in large $CaSO_4$ particles (the form differs substantially from the anhydrite matrix). (Pl. I, micrographs 1 and 2). The $CaSO_4$ envelope (gypsum or anhydrite) has probably protected the KCl against dissolution. Pure KCl particles were observed (Pl. I, micrograph 3); the particles were very clearly affected by dissolution reactions (see e.g. the structure at the bottom of the particle). Another series of Cl-containing particles consist of a complex agglomerate of various mineralogical facies. These contain Na, Mg, Al, Si, P, S, Cl, K and Ca (typical composition in atomic % : 6.9, 8.8, 2.9, 9.0, 2.4, 6.9, 4.4, 2.7 and 11.4 respectively; calculated via ZAF correction procedure; VANDYCK et al., 1984). Apart from chlorides, phosphates and sulphates, some light element containing anions must also be present for electrical neutrality, most probably carbonates and fluorides. The composition of these particles is very imhomogeneous and some parts are enriched in chromium, manganese and iron (Pl. I, micrograph 4). Another example of this type of inclusions is shown in Pl. I, micrograph 5. The dark area consists mainly of Na, S, Cl, K and Ca; although some parts consist of Mg and Si, or Mg, Al and Si. Discrete inclusions of Cr-Fe (probably oxides ?) are also found. The fine "fluffy" crystalline aggregates (white areas) are composed of Cu and S (atomic ratio about 1 : 1). Although the exact formula is difficult to assess due to the massive sulphate containing background, we believe that these crystals are covellite (CuS) which is known to be formed from aqueous solutions at low temperatures and pressures (RICKARD, 1972). Pl. I, micrograph 6 gives a more detailed view of these aggregates. The origin of the
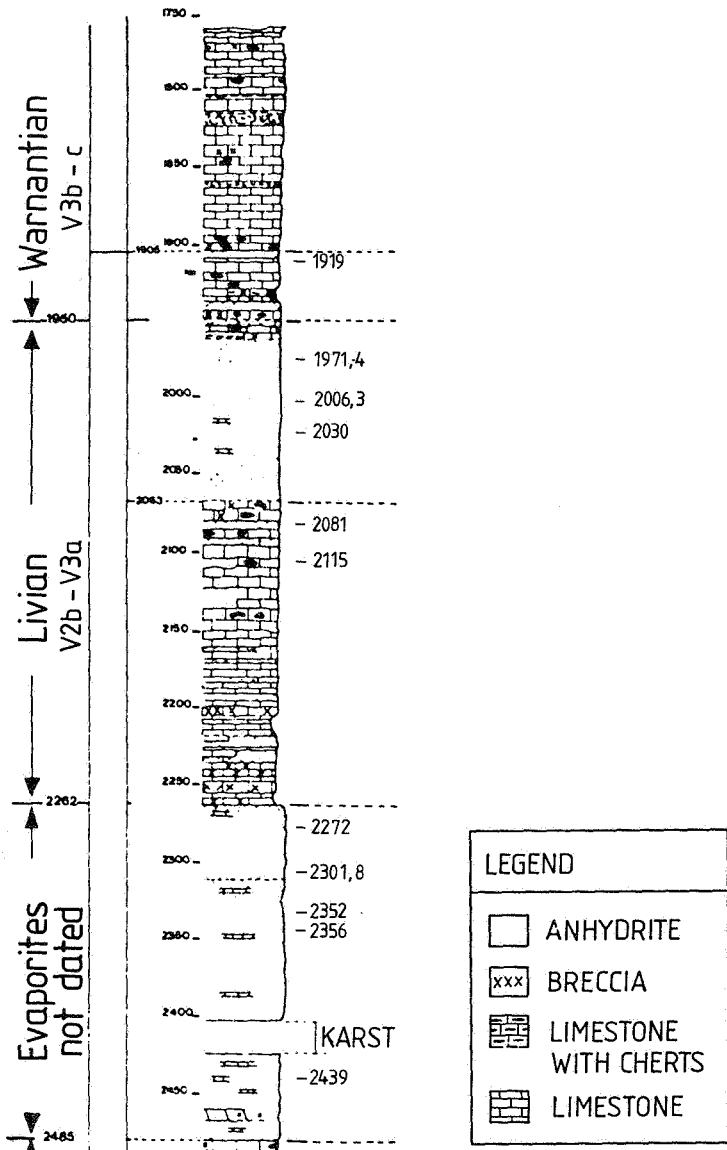
Figure 1. – Location and simplified cross section of Saint-Ghislain drill hole (adapted from ROUCHY *et al.*, 1984).
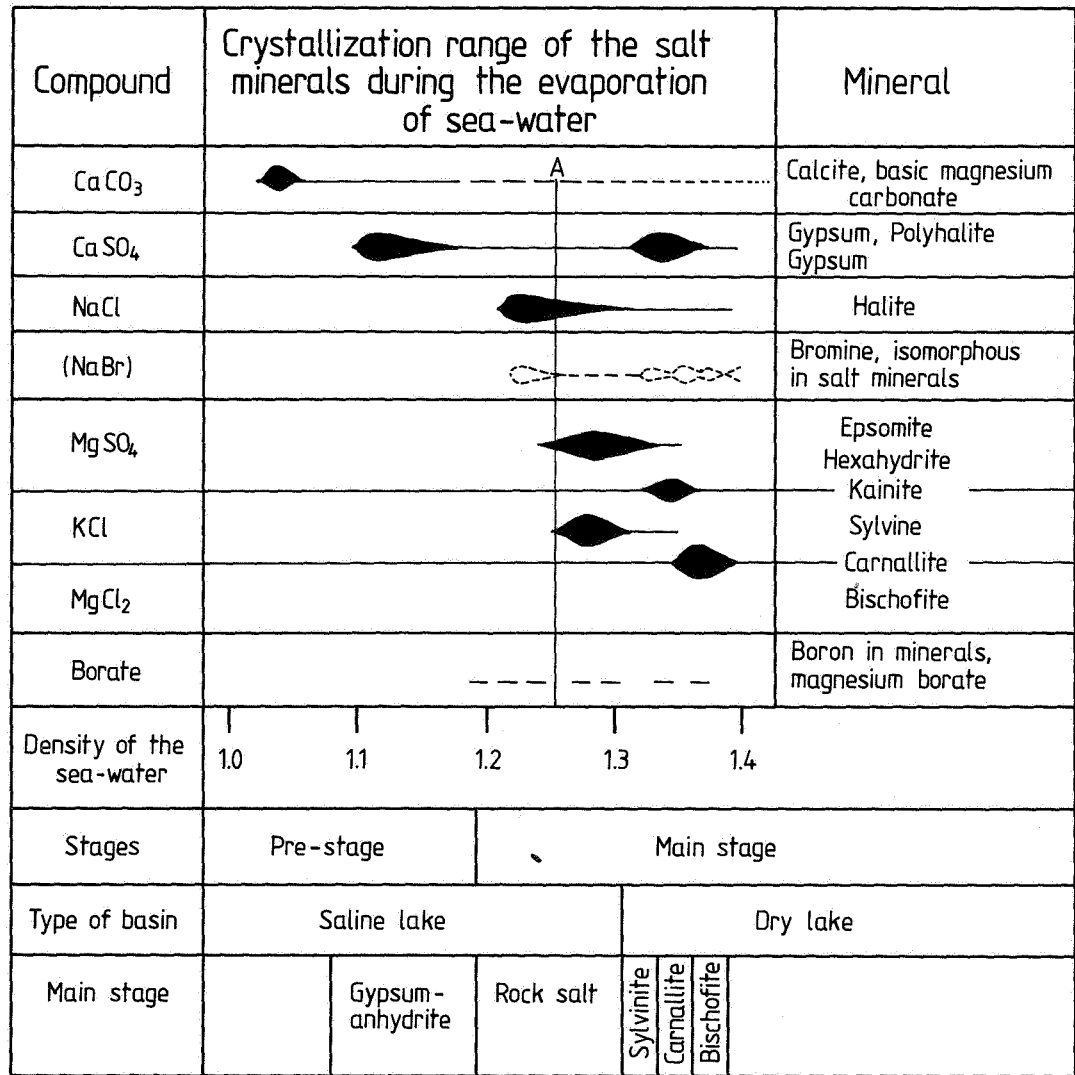
LEGEND

☐	ANHYDRITE
☒	BRECCIA
▦	LIMESTONE WITH CHERTS
▦	LIMESTONE

Compound	Crystallization range of the salt minerals during the evaporation of sea-water	Mineral
CaCO₃		Calcite, basic magnesium carbonate
CaSO₄		Gypsum, Polyhalite Gypsum
NaCl		Halite
(NaBr)		Bromine, isomorphous in salt minerals
MgSO₄		Epsomite Hexahydrite Kainite
KCl		Sylvine Carnallite
MgCl₂		Bischofite
Borate		Boron in minerals, magnesium borate
Density of the sea-water	1.0 1.1 1.2 1.3 1.4	
Stages	Pre-stage	Main stage
Type of basin	Saline lake	Dry lake
Main stage	Gypsum-anhydrite / Rock salt	Sylvinite Carnallite Bischofite

Figure 2. – Evaporitic evolution and precipitation of salts.

TABLE 1. – Concentration levels in Saint-Ghislain anhydrite samples, from various depths (in µg/g); and in Saint-Ghislain thermal water from two sampling campaigns (05/12/1979 and 06/11/1981) (in µg/l).

| | Anhydrites | | | | | | | | | | | St. Ghislain thermal water | | | |
| | | | | | | | | | | | | Solution | | Suspension | |
	1919.	1971.4	2006.3	2030.	2081.	2115.	2272.	2301.8	2352.	2356.	2439.	05/12/79	06/11/81	05/12/79	06/11/81
F	460.	130.	<80.	2100.	<50.	<70.	<70.	<70.	<60.	<70.	760.	2280.	ND	<100.	<100.
Na	22.	18.	40.	140.	9.	<9.	15.	10.	<10.	<9.	<8.	64100.	50900.	21.1	10.0
Mg	970.	260.	1900.	16700.	<340.	440.	1340.	2100.	<350.	320.	190.	25200.	65400.	195.	144.
Al	240.	28.	66.	420.	15.	44.	44.	22.	15.	8.5	13.	380.	38.	298.	349.
Si	4500.	<800.	5000.	5900.	<700.	740.	<700.	<700.	ND	<700.	<800.	19900.	21900.	ND	ND
S	190000.	220000.	210000.	190000.	220000.	210000.	220000.	210000.	210000.	220000.	220000.	371000.	415000.	ND	ND
K	<120.	<120.	<130.	1500.	<140.	<160.	<140.	<130.	ND	<140.	<160.	9200.	7200.	<80.	<80.
Ca	250000.	210000.	200000.	210000.	230000.	230000.	230000.	220000.	260000.	260000.	270000.	397000.	413000.	843.	1180.
Sc	0.039	<0.004	0.014	0.062	<0.004	0.004	0.007	<0.005	<0.004	<0.004	<0.004	0.029	<0.001	0.046	0.048
Ti	22.	18.	<60.	<70.	<70.	<50.	<50.	<50.	<50.	<50.	<50.	<4.	<4.	6.8	13.
V	0.88	0.21	2.0	3.4	<0.6	0.09	0.17	<0.4	<0.4	<0.4	<0.4	<0.07	<0.07	0.23	0.31
Cr	<2.	1.0	<0.9	0.81	<0.8	<0.8	<0.9	1.1	<0.9	<0.9	<0.7	<0.6	<2.	0.25	1.0
Mn	4.6	<5.	<5.	5.2	1.7	<5.	<5.	<5.	<5.	<5.	<5.	83.5	85.0	3.3	3.4
Fe	120.	<50.	<50.	180.	<50.	<40.	<90.	<50.	<50.	<50.	<40.	4190.	4450.	539.	1140.
Zn	<4.	3.6	4.0	<2.	<2.	<2.	<3.	<2.	5.4	<3.	<2.	8.9	<7.	4.0	7.9
Sr	9500.	1500.	8000.	1000.	2000.	1900.	1800.	1300.	1700.	1200.	1500.	6780.	6140.	14.4	<4.
Ba	250.	<30.	<30.	41.	<30.	<30.	<30.	<30.	2400.	<40.	<30.	115.	42.	141.	145.
Pb	33.	4.8	34.	8.6	9.9	12.	4.5	<3.	ND	<3.	<2.	ND	ND	ND	ND

complex Cl and CuS bearing agglomerates may be explained in different ways. According to THIEDE and CAMERON (1978), one can invoke mainly three mechanisms leading to the enrichment in heavy metals (esp. Cu) in an evaporitic sequence :

- interstitial brines can be expelled during compaction; CARPENTIER *et al.* (1974), among others, have suggested that in this case, metals are supplied by an outside source;

- a brine rich in Cu can be generated during conversion of gypsum into anhydrite; BORCHERT and MUIR (1964) have reported that the transformation of 1 m3 of gypsum releases 0.486 m3 of water, that becomes saturated with chlorides through contact with halitic members; this transformation brings important amounts of Cu into solution since primary gypsum contains more metal ions than anhydrite (KROPATCHEV, 1960);

- post-depositional dissolution of evaporites can also release important amounts of metal ions into solution .

The presence of KCl in the Saint-Ghislain evaporites is on the other hand not unexpected. SONNENFELD (1985) has mentioned that evaporites of similar age, found in Canada and Great Britain, mainly contain calcium sulphates, as well as K- and Na- chlorides. The presence of sylvite on the flanks of various subbasins would indicate for this author that :

- organic compounds in the saturated brine impeded carnallite precipitation;

- a density stratification prevented the oxidation and destruction of these organic compounds, this would imply that in deeper layers, a reducing environment

existed so that sulfides could precipitate ; not only CuS but also FeS$_2$ (pyrite) was found (Pl. II, micrograph 7);

- the entrance strait was extremely restricted and the beds were well compacted before Permian sulphatic brines could alter these deposits.

The presence of KCl (sometimes in association with CaSO$_4$) suggests that, at least locally, brines were present within the sequence which testify of an evolution beyond the gypsum and rock salt stages. As is shown in figure 2, the particles mentioned aboved, indicate a stage in evolution beyond point A. Since no remnants of the rock salt stage have been found except cubic calcite pseudomorphs (LECLERCQ, 1980), we must admit that these strata are dissolved and that the hypothesis of DELMER *et al.* (1981) for the formation of the karstic cavities at depth and of the breccias are, at least locally, correct.

The anhydrite sample from 2352 m depth has an anomalous Ba content (2400 µg/g). The baryte mineralization does not seem to be contemporaneous to calcium sulphate deposition but it has invaded and cemented the individual anhydrite particles (Pl. II, micrograph 8), or filled some pre-existing open fractures (Pl. II, micrograph 9). Some of the baryte particles have apparently been affected by tectonic activities similarly as the surrounding matrix (Pl. II, micrograph 10). The baryte mineralization although it appears as massive layers, sometimes occurs as small fanlike particles (some µm in diameter, Pl. II, micrograph 11). The origin of these baryte mineralizations is not clear and many possible sources can be invoked. According to PUCHELT (1967), baryte deposits formed near the earth's surface may be explained by three different

mechanisms :

- evaporation of seawater (Ba and SO_4 originate from the same source);

- injection of a Ba containing hydrothermal solution into seawater (Ba derived from deeper layers, sulphate derived from seawater);

- erosion of clays and carbonates by water, whereby baryte remains because of its low solubility and its high specific weight.

Although all three mechanisms may have played some role here, some remarks can be made referring to the actual situation encountered here. According to PUCHELT (1967), evaporitic baryte is formed only during the very first stage of evaporation, even before calcite/aragonite and gypsum are formed; often, a Ba-rich celestite is formed (celesto-baryte). He also mentions that to obtain a clear precipitation of baryte, the paleomorphology must remain constant over long periods. The baryte encountered in the sample from 2352 m depth is devoid of strontium, so that a formation through simple evaporation of seawater alone is unlikely. The second mechanism, involving a barium containing solution which was injected into the overlying concentrated seawater is more appealing. Baryte mineralizations of the same age are found in other areas nearby (Fleurus). Locally, solutions enriched in barium can be formed through bacterial activity ; sulphates are transformed into sulfides and locally native sulphur is formed. Such processes have been described (ROUCHY et al., 1984) in some anhydrite samples from shallower depth (1919 m) and the native sulphur is shown in Pl. II, micrograph 12. Connate waters from coal measures are also known to be enriched in barium (concentrations up to 200 mg/1 $BaCl_2$ were reported) by the same process. According to ROUCHY et al. (1984), on the other hand, there are indications, at least during Upper Visean (Warnantian) for an interruption in the evaporitic sequence and an influx of fresh seawater into the lagoon. The gypsum present would redissolve whereas the baryte e.g. would remain, so that the third mechanism invoked may also have played a role. Detailed chemical and isotopic analysis can probably elucidate this problem.

ACKNOWLEDGEMENTS.

REFERENCES.

BLOMMAERT, W. (1983) - Trace element geochemistry in geothermal waters and in waters related to ore deposits. *Ph. D. thesis, University of Antwerp,* pp. 285.

BLOMMAERT, W., VANDELANNOOTE, R., SADURSKI, A., VAN 'T DACK, L. and GIJBELS, R. (1983) - Trace element geochemistry of thermal water percolating through a karstic environment in the region of Saint-Ghislain (Belgium). *J. Volcanol. Geotherm. Res.,* 19, 331-348.

BORCHERT, H. and MUIR, R. (1964) - Salt deposits : the origin, metamorphism and deformation of evaporites. *Van Nostrand Co. Ltd., London, Great Britain,* pp. 338.

CARPENTIER, A., TROUT, M.-L. and PICKETT, E. (1974) - Preliminary report on the origin and chemical evolution of the Pb and Zn rich oil field brines in Central Mississippi. *Econ. Geol.,* 69, 942-954.

DELMER, A., LECLERCQ, V., MARLIERE, R. and ROBASZYNSKI, F. (1981) - La géothermie en Hainaut et le sondage de Ghlin. *Ann. Soc. Géol. Nord,* CI, 189-206.

KROPATCHEV, A. (1960) - Minor elements in anhydrites and epigenetic gypsum of the Permian sub-Ural. *Proc. All Union Ass. Mineral., Serie 2,* 89, 589-602.

LAUMONDAIS, A., ROUCHY, J.-M. and GROESSENS, E. (1984) - Importance des formations anhydritiques dinantiennes pour l'interprétation paléogéographique et structurale du domaine varisque d' Europe septentrionale. *C. R. Acad. Sc, Paris, série 2,* 298, 411-414.

LECLERCQ, V. (1980) - Le sondage de Douvrain. *Serv. Géol. de Belgique,* Prof. Paper 170, pp. 51.

PUCHELT, H. (1967) Zur Geochemie des Bariums im exogenen Zyklus. *Sitzungsber. Heidelberger Akad. Wissensch., Math.-Naturw. Klasse,* pp. 205.

RICKARD, D. (1972) - Covellite formation in low temperature aqueous solutions. *Mineral. Deposita,* 7, 180-188.

ROUCHY, J.-M., GROESSENS, E. and LAUMONDAIS, A. (1984) - Sédimentologie de la formation anhydritique viséenne du sondage de Saint-Ghislain. *Bull. Soc. Belge de Géologie,* 93, 105-145.

SONNENFELD, P. (1985) - Carboniferous evaporites along Canada's continental shelves. *Abstr. Symp. Pre-Permian evaporites of Europe. May 09-10, 1985, Brussels (Belgium).*

THIEDE, D. and CAMERON, E. (1978) - Concentration of heavy metals in the Elk Point evaporites sequence, Saskatchewan. *Econ. Geol.,* 73, 405-415.

PLATE I

Micrograph 1: KCl inclusions (arrowheads) in $CaSO_4$ matrix (sample from 2030 m depth)
bar = 10 µm.
Inclusion de KCl (flèches) dans une matrice de $CaSO_4$ (échantillon pro-
venant d'une profondeur de 2030 m) barre = 10 µm.

Micrograph 2: KCl inclusions (arrowheads) in $CaSO_4$ matrix (sample from 2030 m depth)
bar = 10 µm.
Inclusion de KCl (flèches) dans une matrice de $CaSO_4$ (échantillon_pro-
venant d'une profondeur de 2030 m) barre = 10 µm.

Micrograph 3: KCl particles (A) (sample from 2030 m depth) bar = 10 µm.
Particule de KCl (A) (échantillon provenant de 2030 de profondeur)
barre = 10 µm.

Micrograph 4: Complex Na - Mg - Al - Si - P - S - Cl - K - Ca containing particle
(sample from 2030 m depth) bar = 10 µm.
Inclusion complexe à Na - Mg - Al - Si - P - S - Cl - K - Ca (échantil-
lon provenant d'une profondeur de 2030 m) barre = 10 µm.

Micrograph 5: Complex Na - S - Cl - K - Ca containing particle (sample from 2030 m
depth) bar = 100 µm.
region A : Mg - Al - Si
region B : Mg - Si
region C : Cr - Fe
region D : S - Cu
Inclusion complexe à Na - S - Cl - K - Ca (échantillon provenant d'une
profondeur de 2030 m) barre = 100 µm.
région A : Mg - Al - Si
région B : Mg - Si
région C : Cr - Fe
région D : S - Cu

Micrograph 6: Close-up view of CuS crystals (sample from 2030 m depth) bar = 10 µm.
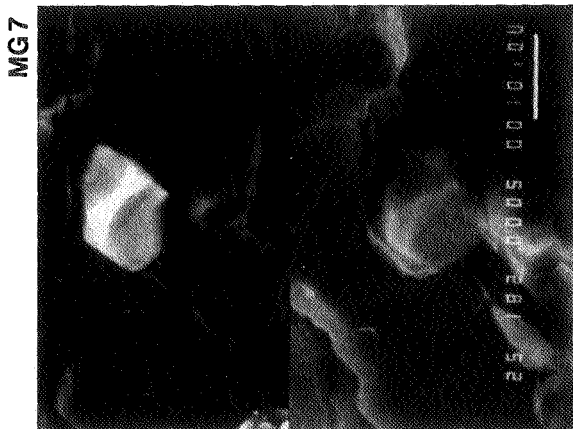Vue élargie des CuS cristaux (échantillon provenant d'une profondeur
de 2030 m) barre = 10 µm.
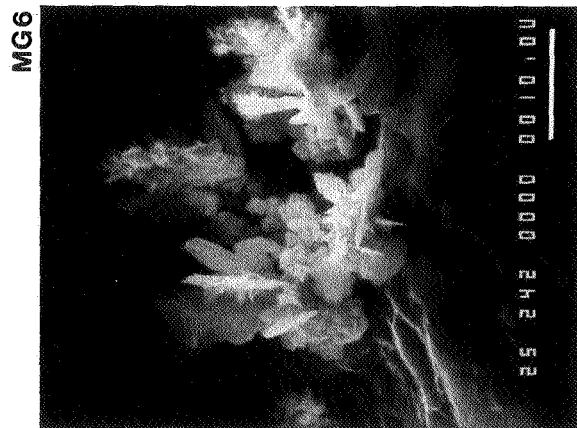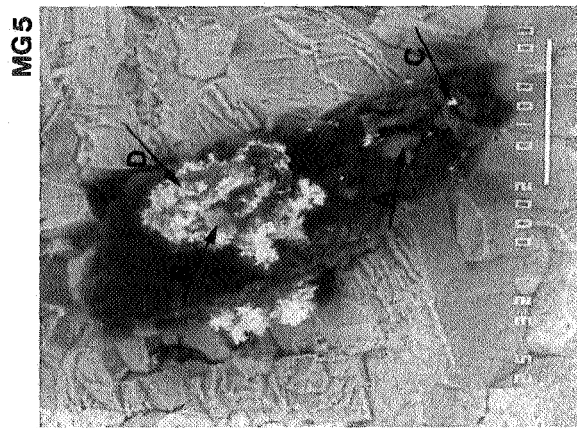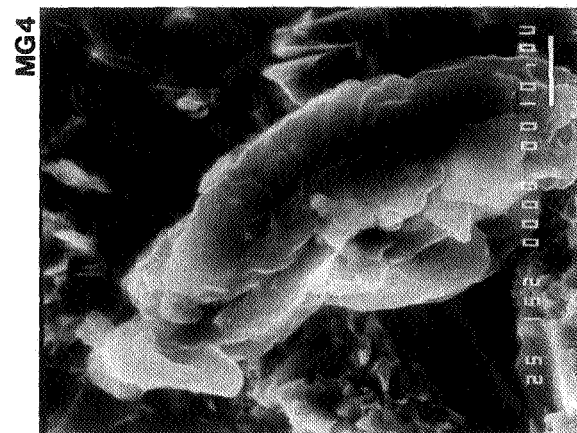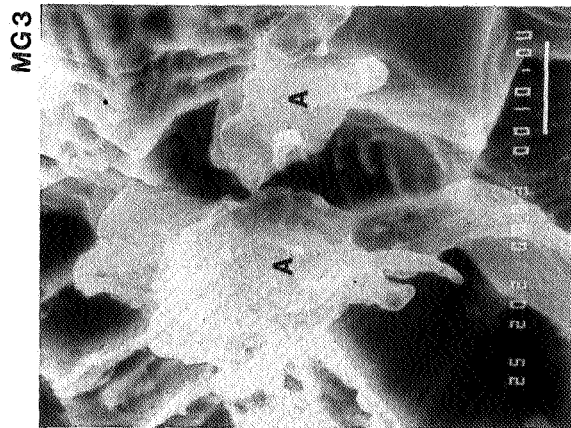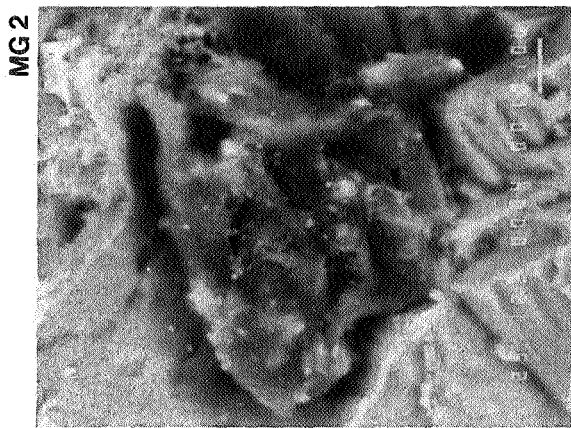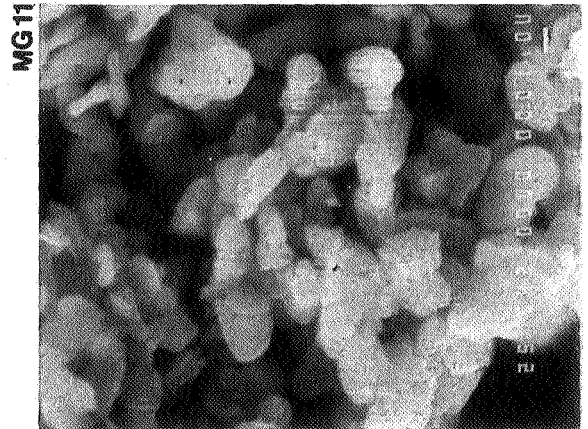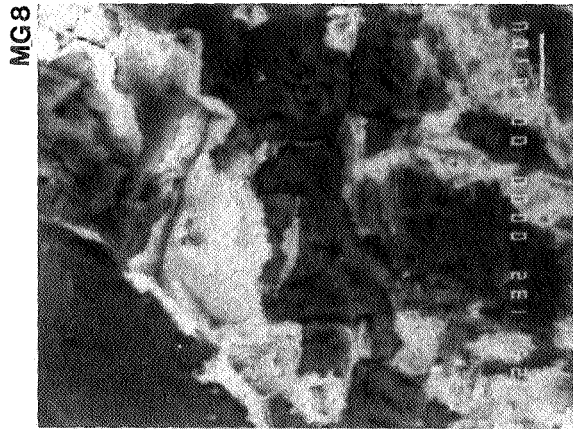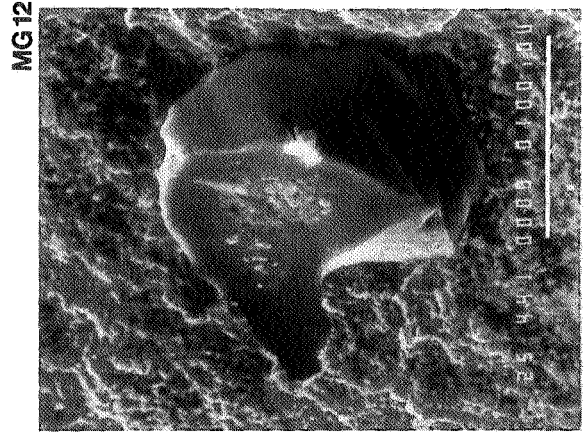
PLATE II

Micrograph 7: Pyrite crystal (sample from 2030 m depth) bar = 10 μm.
Inclusion de pyrite (échantillon provenant d'une profondeur de
2030 m) barre = 10 μm.

Micrograph 8: Baryte cementation (light areas) inbetween anhydrite (sample from
2352 m depth) bar = 10 μm.
Cimentation barytique (régions claires) dans une matrice an-
hydritique (échantillon provenant d'une profondeur de 2352 m)
barre = 10 μm.

Micrograph 9: Baryte (arrowheads) filling open fracture (sample from 2352 m
depth) bar = 10 μm.
Barytine (flèches) remplissant une fissure (échantillon provenant
d'une profondeur de 2352 m) barre = 10 μm.

Micrograph 10: Baryte inclusion (light area) (sample from 2352 m depth)
bar = 100 μm.
Inclusion à barytine (régions claires) (échantillon provenant
d'une profondeur de 2352 m) barre = 100 μm.

Micrograph 11: Fan-like baryte particles (sample from 2352 m depth) bar = 1 μm.
Particule de barytine en forme d'évantail (échantillon provenant
d'une profondeur de 2352 m) barre = 1 μm.

Micrograph 12: Native sulphur particle in a carbonate matrix; arrowhead points to
celestite (sample from 1919 m depth) bar = 100 μm.
Inclusion de soufre natif dans une matrice carbonatée; la flèche
indique une particule de celestine (échantillon provenant d'une
profondeur de 1919 m) bar = 100 μm.

VANDYCK, P., STORMS, H. and VAN GRIEKEN, R.
    (1984) - Automated quantitative
    electron microprobe analysis of parti-
    culate material. *J. Phys.*, 45, C2
    781-784.

VAN GRIEKEN, R., VAN 'T DACK, L., COSTA DANTAS, C.
    and DA SILVEIRA DANTAS, H. (1979) -
    Soil analysis by thin film energy-
    dispersive X-ray fluorescence. *Anal.
    Chim. Acta*, 108, 93-101.

MG9

MG8

MG7

MG12

MG11

MG10

109